

# Physical Properties of Non-Stoichiometric Sintered TiO Ceramics

Katsuya KUDAKA\* Kiyokata IIZUMI\*\* and Shinya WATANABE\*\*\*

Non-stoichiometric sintered TiO ceramics were produced by sintering at 1350°C in a vacuum of  $10^{-4}$  Torr, starting from the mixed powder of titanium oxide and titanium as raw materials.

The TiO phase obtained was mainly cubic, but it contained complex ordered lattice structure phase only a little in the composition range between  $\text{TiO}_{0.94}$  and  $\text{TiO}_{1.02}$ . Some physical properties, such as mechanical, electrical and optical properties, and some factors governing the microstructure of the sintered bodies, such as mean crystal size, lattice strain and apparent density, were measured and related with the composition of non-stoichiometric TiO phase.

Many oxides, carbides and nitrides of the group IVa and Va metals crystallize with the simple NaCl type structure at composition of about MX. These compounds generally have wide ranges of non-stoichiometry. In particular, the phase of TiO has long been known to exist over a wide range of composition depending on temperature, e. g. from  $\text{TiO}_{0.9}$  to  $\text{TiO}_{1.25}$  at temperatures below about 990°C<sup>1)</sup>. An important feature of this phase, which has been deduced from a comparison of pycnometric and x-ray densities, is that its crystal structure has varying proportions of titanium and oxygen vacancies and even in the equiatomic composition about 15% of both titanium and oxygen sites are vacant<sup>1)</sup>. Although several properties of non-stoichiometric TiO solidified from the

melt, have been studied in detail<sup>2)</sup>, the study of non-stoichiometric TiO sintered bodies have not been reported. This work shows the effects of the continuous variation in oxygen concentration (O/Ti ratio) on the some physical properties and some factors governing the microstructure of non-stoichiometric TiO sintered bodies.

## Experimental

Anatase of particle size  $<0.1\mu\text{m}$  and titanium of particle size  $<1\mu\text{m}$  were mixed in the compositions as shown in Table I by ball milling in hexane for 24 h, formed at a pressure of 1 t/cm<sup>2</sup>, sintered at 1000°C in a vacuum of  $10^{-4}$  Torr for 1 h, crushed by ball milling in hexane for 48 h and then the powder was formed at a pressure of 1 t/cm<sup>2</sup> and sintered at 1350°C in a vacuum of  $10^{-4}$  Torr for 1 h<sup>3)</sup>. In the sintering processes, the specimens were placed in graphite boats in contact with green

\* Professor, Department of Industrial Chemistry

\*\* Research Associate, Department of Industrial Chemistry.

\*\*\* Japan Color Research Institute.

(Received Oct. 4, 1980)

**Table I.** Mixing ratio of TiO<sub>2</sub> and titanium.

Sample No.	TiO <sub>2</sub>	Ti	O/Ti <sup>a)</sup>
1	1.0	1.2	0.91
2	1.0	1.1	0.95
3	1.0	1.0	1.00
4	1.0	0.9	1.05
5	1.0	0.8	1.11

a) Atomic ratio of oxygen to titanium at mixing.

compacts of titanium powder which were used as oxygen buffers<sup>4)</sup>.

The microstructure of the sintered bodies was observed under an optical microscope after etching the polished surface with the mixed solution of hydrogen peroxide and fluoric acid. X-ray diffraction with Ni-filtered CuK $\alpha$  radiation was used to identify the products, measure the lattice parameters of the TiO phases and estimate the residual strain in the TiO lattices. The apparent density of the sintered bodies was measured by means of the water displacement method. The electrical resistance of the samples was measured with the 4-probe circuit at room temperature (about 25°C). The bending strength and the micro-vicker's hardness of the samples were also measured. The relative spectral reflection curves of the polished surfaces of the sintered bodies were measured with a color analyser to calculate the color specifications and the Munsell value of the specimens.

## Results and Discussion

### X-ray analysis

Table II shows the identified phases in the sintered bodies, the lattice constants of the TiO phases and the half width of the TiO (331) lines obtained by x-ray diffraction. Table III shows the mixing ratios expressed in atomic

ratio and the estimated compositions of the TiO phases, obtained from the lattice constants and the data<sup>5)</sup> of non-stoichiometric TiO solidified from the melts, expressed in O/Ti ratio and chemical formula. Most of the identified phases were cubic TiO, while weak peaks of the complex ordered structure<sup>\*1</sup> of TiO phase were observed in the samples of No.1 and No.2.

In Table III, the O/Ti ratios of the TiO phases differ from the mixing ratios in the direction of increase. It is possibly caused by the diffusion of oxygen from the atmosphere. Fig.1 (a) shows the relationship between the lattice strain<sup>\*2</sup> of the cubic TiO, obtained

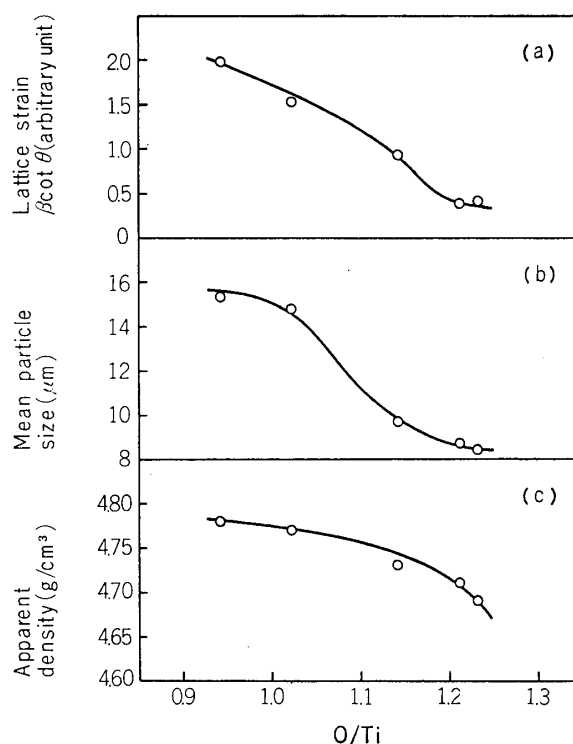


**Fig. 1.** Relationships between some factors governing the microstructure of TiO sintered bodies and composition of TiO phase.

\*1 It is assumed as monoclinic TiO<sup>1)</sup>.

\*2 The line-broadening cannot be considered to be due to grain size because the grain size in these sintered bodies were 5~19  $\mu$ m as shown later and therefore it is assumed to be wholly due to the lattice strain.

**Table II.** The results of X-ray analysis.

Sample No.	Identified phase	Lattice constant of TiO (cub) (Å)	Half width of (331) line (°)
1	TiO (cub) <sup>a)</sup> TiO (comp) <sup>b)</sup> *	4.187	1.32
2	TiO (cub)      TiO (comp)	4.182	1.01
3	TiO (cub)	4.176	0.62
4	TiO (cub)	4.171 <sub>9</sub>	0.25
5	TiO (cub)	4.170 <sub>4</sub>	0.28

a) TiO phase with NaCl structure.

b) TiO phase with complex ordered lattice structure.

\* weak relative intensity.

**Table III.** Composition of TiO phase estimated from the results of X-ray analysis.

Sample No.	Mixing ratio (O/Ti)	Composition of <sup>a)</sup> TiO phase (O/Ti)	Estimated chemical formula
1	0.91	0.94	TiO <sub>0.94</sub>
2	0.95	1.02	TiO <sub>1.02</sub>
3	1.00	1.14	TiO <sub>1.14</sub>
4	1.05	1.21	TiO <sub>1.21</sub>
5	1.11	1.23	TiO <sub>1.23</sub>

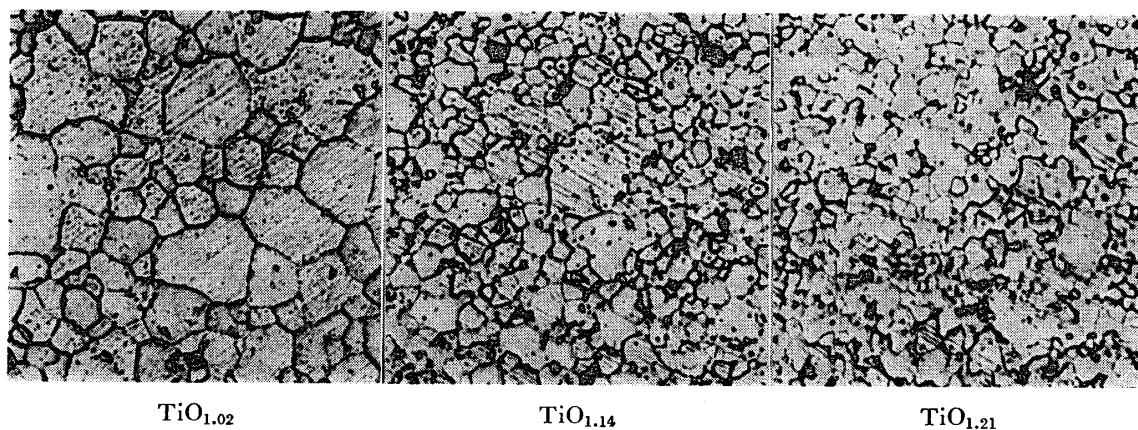
a) These values were estimated with the measured values of lattice constant and the data of Takeuchi et al.<sup>4)</sup> on TiO.

from the broadening of the diffraction lines, and the composition of the cubic TiO phase. As the oxygen content in the TiO phase decreases, the complex ordered lattice of TiO phase which attributes to the lattice strain of the TiO phase slightly appears.

#### Crystal size

The optical photographs of TiO<sub>1.02</sub>, TiO<sub>1.14</sub>

and TiO<sub>1.21</sub> sintered bodies are shown in Fig. 2. Fig. 1 (b) shows the relationship between the mean crystal size measured in the photographs by Fullman's method<sup>6)</sup> and the composition of the TiO phases. As the oxygen content in the TiO phase decreased, crystal growth was accelerated probably due to the increase in the diffusion rate. It corresponds with the report<sup>5)</sup>

**Fig. 2.** Microphotographs of TiO sintered bodies ( $\times 400$ ).

**Table IV.** Apparent density and porosity of TiO sintered bodies.

Sample No.	Composition of TiO phase (O/Ti)	Apparent density (g/cm <sup>3</sup> )	True density <sup>a)</sup> (g/cm <sup>3</sup> )	Porosity <sup>b)</sup> (%)
1	0.94	4.78	5.00	4.4
2	1.02	4.77	4.97	4.0
3	1.14	4.73	4.93	4.1
4	1.21	4.71	4.92	4.3
5	1.23	4.69	4.88	3.9

a) The values were estimated with composition of TiO phase and the data of Takeuchi et al.<sup>4)</sup>

b) Porosity = (1 - apparent density / true density) × 100.

that as the oxygen content decreases, the vacancy concentration (the sum of Ti and O vacancies) increases.

#### Apparent density

Table IV shows the apparent densities of the sintered bodies, the true densities estimated from the previous data<sup>5)</sup> about non-stoichiometric TiO solidified from the melts, and the porosities calculated from the two kinds of densities. The relationship between the apparent density of the sintered body and the composition of the TiO phase is shown in Fig. 1 (c). As the oxygen content increases, the apparent density decreases, while the porosity of the sintered bodies remains almost constant.

#### Hardness and bending strength

As shown in Fig. 3 (a) and (b), both the micro-vicker's hardness and the bending strength of the sintered bodies increase, as the oxygen content decreases. This is probably due to the hardening of the TiO crystal lattice which corresponds with the increase of the lattice strain in TiO phase as shown in Fig. 1 (a). Therefore in this study it can be assumed that lattice strain was more effective parameter for the hardness of the TiO sintered bodies than crystal size.

#### Electrical resistance

As shown in Fig. 3(c), the electrical resistance

of the sintered bodies at 25°C is almost constant in the composition range from TiO<sub>0.94</sub> to TiO<sub>1.02</sub>, whereas it increases with the oxygen content in TiO phase in the composition of O/Ti > 1.02. This tendency nearly corresponds with that

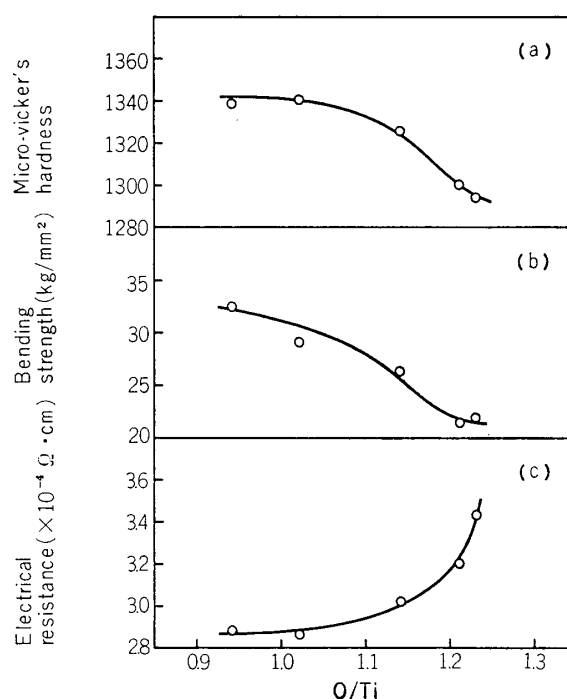


**Fig. 3.** Relationships between physical properties of TiO sintered bodies and composition of TiO phase.

of non-stoichiometric TiO solidified from the melt<sup>7)</sup>. That is, in the composition of O/Ti > 1.02, as the oxygen content increases, the

Table V. Color specification and Munsell value of TiO sintered bodies.

Sample No.	Composition of TiO phase (O/Ti)	Y (%)	X	Y	Munsell value
1	0.94	50.0	0.355	0.361	2.5 Y 7.5/3.0
2	1.02	48.1	0.363	0.368	2.5 Y 7.3/3.2
3	1.14	46.6	0.373	0.373	2.5 Y 7.0/3.7
4	1.21	42.2	0.386	0.386	2.5 Y 6.9/4.9
5	1.23	40.6	0.396	0.394	2.5 Y 6.8/5.3

number of valence electrons per unit lattice<sup>\*3</sup> decreases with the character of the metallic bond. The measured values of the electrical resistance show a good agreement with the electrical data of sintered TiO ceramics by A. A. Samsonov<sup>8)</sup>.

### Color

The color of the polished surfaces of the sintered TiO ceramics can be roughly called golden. Table V shows the color specification and the Munsell value of the sintered TiO, obtained from the relative spectral reflection

curves shown in Fig. 4. As the oxygen content in the TiO phase increases, the value decreases and the chroma increases, whereas the hue is almost constant (2.5 Y) in the composition of O/Ti = 0.94~1.23. It corresponds with the decrease in the character of metallic bond.

### Conclusion

Non-stoichiometric TiO sintered bodies were produced by sintering at 1350°C in a vacuum of  $10^{-4}$  Torr, starting from the mixed powder of titanium oxide and titanium as raw materials. Some physical properties, such as mechanical, electrical and optical properties and some factors governing the microstructure of the sintered bodies, such as mean particle size, lattice strain and apparent density were measured.

The following results were obtained. (1) The TiO phase obtained is mainly cubic, but it contains complex ordered lattice structure phase only a little in the composition range between  $\text{TiO}_{0.94}$  and  $\text{TiO}_{1.02}$ . (2) As the oxygen content in TiO phase decreases, the crystal size, the apparent density and the lattice strain increase. (3) As the oxygen content in TiO phase decreases, the hardness and the bending strength of the sintered bodies increase. The facts are assumed to be the effects of the lattice strain. (4) The electrical resistance of the sintered bodies is almost constant in the composition range of  $\text{TiO}_{0.94} \sim$

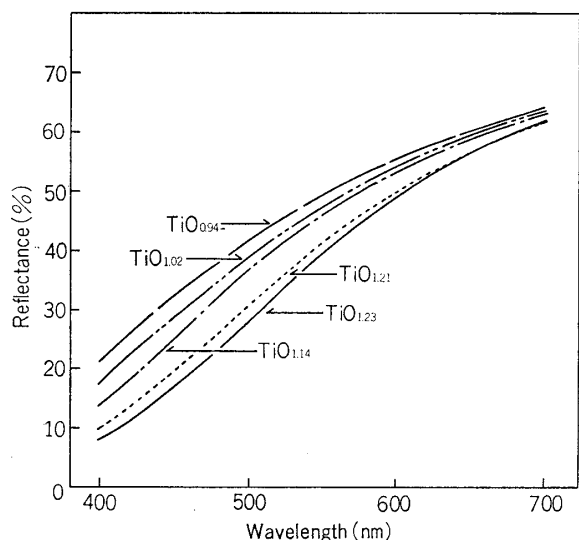


Fig. 4. Relative spectral reflection curves of non-stoichiometric sintered TiO ceramics.

<sup>\*3</sup> The number of valence electrons per unit lattice of perfect crystal  $\text{TiO}_{1.00}$  is ten, while that of real crystal  $\text{TiO}_{1.00}$  is 8.5 because the real crystal contains vacancies of about 15%.

TiO<sub>1.02</sub>, whereas it increases with the oxygen content in TiO phase in the composition range of O/Ti>1.02. (5) According to the color analysis of the polished surfaces of the sintered bodies, as the oxygen content in TiO phase increases, the value decreases and the chroma increases, whereas the hue is almost constant (2.5Y) in the compositions of O/Ti=0.94~1.23.

#### Acknowledgment

The authors are indebted to Dr. K. Kamimura of Department of Electronics and Mr. K. Arai of Department of Image Science for contributing measurements of electrical resistance and relative spectral reflection curves respectively.

#### References

- 1) D. Watanabe, J. R. Castles, A. Jonstons and A. S. Malin, *Acta Cryst.*, **23**, 307 (1967).
- 2) K. Suzuki, "Non-stoichiometric Metallic Compounds", Maruzen, (1975), p. 1.
- 3) K. Kudaka, T. Hanazawa and H. Takai, *Yogyo-Kyokai-shi*, **86**, 41 (1978).
- 4) T. J. Reed, "The chemistry of Extended Defects in Non-metallic Solids", North-Holland Publishing Co., (1970), p. 21.
- 5) S. Takeuchi and K. Suzuki, *Nihon-Kinzoku-Gakkai-Shi*, **31**, 611 (1967).
- 6) R. L. Fullman, *J. Metals*, **5**, 477 (1953).
- 7) K. Suzuki and S. Takeuchi, "Ferrites, Proceeding of the International Conference", ed. by Y. Hoshino, S. Iida and M. Sugimoto, Univ. of Tokyo Press, (1971), p. 279.
- 8) A. A. Samsonov and A. G. Rustamov, *Soviet Physics-Solid State*, **5**, 877 (1963).